Hindawi
Advances in Materials Science and Engineering
Volume 2024, Article ID 6652973, 15 pages
https://doi.org/10.1155/2024/6652973

Research Article

A Hybrid Nondominant-Based Genetic Algorithm (NSGA-II) for Multiobjective Optimization to Minimize Vibration Amplitude in the End Milling Process

Mahesh Gopal,[1] **Endalkachew Mosisa Gutema**,[1] **Hirpa G. Lemu**,[2] **and Jaleta Sori**[1]

[1]*Department of Mechanical Engineering, College of Engineering and Technology, Wollega University, Nekemte, P.O. Box 395, Ethiopia*
[2]*Department of Mechanical and Structural Engineering and Materials Science, Faculty of Science and Technology, University of Stavanger, N-4036 Stavanger, Norway*

Correspondence should be addressed to Hirpa G. Lemu; hirpa.g.lemu@uis.no

Received 19 September 2023; Revised 8 December 2023; Accepted 23 December 2023; Published 3 January 2024

Academic Editor: Rong Lu

Aluminium is a noncorrosive, lightweight material used to fabricate parts for the aerospace, automobile, and construction industries. Due to the low-temperature resistance, more heat is generated. At the same time, in machining, tremendous efforts are taken to keep friction and chatter to a minimum and to attain better quality and perfect output, and also more attention is required while selecting the machining process parameters. Spindle speed, rate of feed, radial and axial depth of cut, and radial rake angle of the tool are the parameters utilized to machine aluminium 6063 using the HSS tool on CNC milling to estimate spindle and worktable vibration using a prediction model. In this study, the design of the experiment of the response surface methodology approach is used to create a second-order statistical equation for experimentation with the Design-Expert v12 software. The performance characteristics are analyzed using the ANOVA method. The spindle speed achieved the lowest vibration between 2000 and 3000 rpm. Next, axial and radial depths were the most vibration-affecting parameter compared to the rate of feed and radial rake angle of the tool. To find the best feasible response, the nondominant sorting genetic algorithm II (NSGA II) approach was trained and tested using MATLAB software. Using a Pareto-optimal technique, the optimum worktable vibration ranged from 0.00284 to 0.00165 mm/s^2, whereas the spindle vibration ranged from 0.02404 to 0.01336 mm/s^2. The predicted values were found to be in an excellent argument when Pareto-optimal solutions are used.

1. Introduction

In recent years, manufacturers have focused on predicting machining process parameters to minimize machining processes and to meet customer expectations of low cost and high quality. Furthermore, predicting machining parameters that can reduce machine and tool vibrations and produce high-quality materials is crucial in machining. Some discrepancies existed between the simulated and measured cutting forces inside each cycle due to self-excited vibration during the milling process [1]. Nowadays, vibration analysis gives a great interest to researchers. Significant efforts are needed to monitor and minimize vibrations in cutting tools and machines. To measure and analyze the vibrations, vibration testers, piezoelectric sensors, micro-electromechanical sensors, proximity probes, laser Doppler vibrometers, and accelerometers are used.

The cutting process was performed using a cubic boron nitride (CBN) end mill cutter and AISI-D3 steel material to study the relationship between the wear in the tool and vibration amplitude. Vibration is commonly measured using an accelerometer. The author [2] found that increased tool wear is caused by an increase in vibration amplitude at high peak frequencies.

The vibration amplitude signal significantly increases when the flank is substantially damaged. This results from wearing one flute in an experiment employing accelerometers while milling mild steel workpieces with HSS four-flute

end mills to monitor tool wear evolution [3]. To increase steel machinability, the influence of vibration on surface unevenness and tool wear was estimated using an end milling process. Surface unevenness and wear in the tool can be reduced using two-dimensional vibration-assisted microend milling (2-D VAMEM) [4]. Sivasakthivel et al. [5] measured the acceleration amplitude using a fast Fourier-transform (FFT) analyzer of Al 6063 material, and the tools used for experimentation were HSS end mill. The input parameters considered are the helix angle of a cutting tool, spindle speed, feed rate, and the axial and radial depth of cut and found that the tool's helix angle is the most relevant parameter in lowering vibration amplitude. The research reported by Shen et al. [6] experimented using aluminium alloys to minimize the ultrasonic vibration. The bottom region of the slot and the vertical sidewall region of the place were studied in a slot-milling machine experiment to decrease surface unevenness. According to the *F*-test, the most influential factors are spindle speed and the rate of feed. Surface unevenness and vibration amplitude are minimized considering spindle speed, axial cutting depth, feed, and heating temperature as input parameters are optimized using the analysis of variance (ANOVA) approach with the design of experiment (DoE) of response surface methodology (RSM) and the desired function approach. In the vertical milling center experiment, surface morphology and vibration were assessed using a ball-end-coated carbide insert. According to Amin et al. [7], the temperature and cutting speed have the greatest influence on the resulting surface quality and maximum vibration amplitude. Experiments were performed using AISI H13 steel with a TiAlN tool to measure the tool's surface roughness, tool wear, and vibration and concluded that wear in the tool and surface roughness depend primarily on tool instability [8]. A finite element model is developed to find the vibration on milling machines. The experimental work was completed, and data were obtained using statistical analysis, which revealed that surface roughness is mostly impacted by the dynamical features of the cutting tool [9].

Milling machine experiments were performed on C45E4 steel; optimization was carried out using a Gaussian process regression model, which analyzes surface roughness while taking into account tool vibration. The Gaussian process regression (GPR) model was used to forecast surface roughness, and the results indicated that vibration in the tool is also an important factor that impacts surface quality [10]. The researcher [11] designed a mathematical model using the RSM optimization technique to measure tool vibration, surface quality, and tool wear during milling EN31 tools. The conclusion stated that the feed is the influencing element impacting surface quality and cutting speed affects the tool. The vibration analysis experiments were conducted by Sivasakthivel et al. [12] on tool holders and workpiece holders to machine aluminium Al 6351 material considering the rake angle, nose radius, cutting speed, feed rate, and depth of cut. The regression model was developed, optimization was performed using a genetic algorithm, and the nose radius showed a negative value during sensitivity analysis. The author [13] stated that tool life, quality of machined products, and functional behavior are primarily affected by vibration. Studies have been conducted using magnetic rheological fluid dampers to suppress vibration using AISI 4340 steel with 45HRC indexable inserts on milling machines. As a consequence, the damper decreases tool vibration while increasing cutting performance. The cutting resistance and vibration are measured by [14] during the simulation experiment using finite element modeling. Experiments have shown that improved tool orientation has been found to minimize machining distortion and increase surface quality.

Vibration analysis and Hilbert–Huang transforms (HHTs) were used to monitor the condition of the milling machine and compare the results with FFT. As a result, HHTs revealed the difference in cutting edge due to its high time/frequency resolution, and the cutting fluid increased the vibration damping in the milling machine [15]. A 55NiCrMoV6 steel ball-end milling machine experiment measured the cutting resistance and vibration. Surface roughness topography was investigated utilizing the signal-to-sound (S/N) ratio and grey rational analysis (GRA) with the surface angle of inclination and tool overhang taken into account. As a result, the angle of inclination and tool overhang have a substantial impact on the produced force and vibration values. Selecting the best tilt angle and tool overhang will decrease surface quality [16]. Vibrations that occur when a flat-end cutter arrives at a workpiece during machining can have a significant impact on the quality of the finished part, tool life, and machining efficiency. To address this issue, a combination of modeling, simulations, and experiments can be used to understand, predict, and mitigate these vibrations [17]. The experiments were designed using signal processing technology to measure the acceleration signals in spindle vibrations of tools generated during the end mill process. The protective chamfer, along with a relatively high rake angle, is a successful criterion to minimize the amplitude of vibration under most cutting settings [18].

At various vibration amplitudes and cutting velocities, compression studies were conducted on the surface integrity of the Ti-6Al-4V end mill. Surface roughness values increase as the cutting rate and vibration amplitude increase, resulting in a considerable microvibration texture in rotary ultrasonic elliptical end milling (RUEEM) in the form of burrs divided into machined surfaces [19]. Lin et al. [20] generated a regression model to forecast the surface roughness of Al 6061 materials and optimized using artificial neural networks to measure vibration during end mills based on cutting factors. Estimating prediction accuracy can be ensured by emphasizing the results of the developed prediction model derived from cutting conditions that consider machining stability. A milling experimental study was conducted by a researcher [21] to improve the surface unevenness of AISI 52100 bearing steel and the impact level of the workpiece. The researcher [22] evaluated the surface roughness in the slot end-mill process with a variable helix angle for aluminium machining. A statistical analysis was conducted to measure surface roughness and proved that variable helix angles can produce much higher surface

roughness quality than standard helix angle tools. The experimental investigation of cutting vibration during microend-milling of a straight groove involves studying and measuring the vibrations generated during the machining process. Based on the results, spindle speed is the most critical characteristic that causes cutting vibration [23].

Using the Taguchi technique, cutting factors were studied. Experiments have shown that cutting speed and tooth contact feed were the most inducing factors affecting the surface of the material in both cases. Regression and ANOVA techniques were utilized to anticipate the acceleration amplitude. Based on the results, cutting speed has a significant influence on the vibration amplitudes [24]. The purpose of the study was to improve the machinability of AISI H13 material and identify the ultrasonic vibrations caused in the end milling process. The results revealed a continual change in mechanical loading caused by the tool's vibratory motion, resulting in a decrease in cutting forces [25]. Implementing a stacked generalization ensembles model for milling tool wear state recognition by vibration signal analysis can enhance the efficiency and safety of machining processes by enabling proactive maintenance and tool replacement, thereby minimizing downtime and optimizing tool usage [26].

In general, vibration is undesirable phenomenon, resulting in unpleasant motions and dynamic stresses, and also affects machining performance, particularly surface finish and tool life. A survey of the previously published literature indicates that there are a few publications published on optimizing the parameters impacting vibration characteristics during the milling process of aluminium 6063. Furthermore, none of the studies use experimental analysis to evaluate spindle and worktable vibration under real-world conditions, including the spindle speed, feed rate, axial depth of cut, radial depth of cut, and radial rake angle of the tool. The RSM, ANOVA statistical analysis, and nondominated sorted genetic algorithm (NSGA-II) heuristic approaches were also performed to optimize the milling parameters.

2. Development of a Mathematical Model

Because the first-order model tends to be inadequate for a curved response surface, the second-order model is recommended to approximate a section of the genuine response surface with curvature. All of the terms from the first-order model, as well as quadratic and cross-product terms, are included in the second-order model. Second-order models depict quadratic surfaces like minimum, maximum, ridge, and saddle. Thus, a second-order linear difference equation is a mathematical equation that represents the connection between consecutive terms in a series. A quadratic polynomial form and second-order model can be represented as follows [5]:

$$y'' = \beta_0 x_0 + \beta_1 x_1 + \beta_2 x_2 + \beta_3 x_3 + \beta_{11} x_1^2 + \beta_{22} x_2^2 + \beta_{33} x_3^2 + \beta_{11} x_1 x_2 + \beta_{12} x_1 x_3 + \beta_{14} x_2 x_3, \quad (1)$$

where y'' is the approximated response given in the second-order equation, β_0 is the regression equation's free term coefficients, x_0, x_1, ... are linear factors, x_{11}, x_{22}, ... are the quadratic terms, and x_{12}, x_{13}, ... are the interaction terms.

The polynomial coefficients are determined using the multiple regression method. The coefficients are calculated using the statistical software Design-Expert v12.

3. Experimental Design

In the present work, the spindle speed, feed rate, axial depth of cut, radial depth of cut, and radial rake of the cutting tool have been considered as the process parameters to measure spindle and worktable vibration.

RSM is a set of mathematical and statistical tools used to analyze situations like the one given using an empirical model and also the most informative method of analysis of the result of a factorial experiment. It is a technique that graphs the results of polynomial regression studies in three dimensions to offer a sophisticated perspective of correlations between combinations of two predictor variables and an outcome variable.

The output response vibration on the spindle and worktable may be represented as a function of process parameters such as the spindle speed (N), rate of feed (f_z), axial depth of cut (a_p), radial depth of cut (a_e), and radial rake angle of the tool (γ).

Using these parameters, the objective is to get the best possible answer for the machine performance. Similarly, several studies have theoretically anticipated output responses using equation (27):

$$A = cN^{k_1} f_z{}^{k_2} a_p{}^{k_3} a_e{}^{k_4} \gamma^{k_5}, \quad (2)$$

where A is the actual acceleration amplitude response (mm/s^2), N is the spindle speed (m/min), f_z is the rate of feed (mm/rev), a_p is the cutting depth (axial) (mm), a_e is the cutting depth (radial) (mm), and γ is the rake angle of tool (radial) (degree).

The model parameters are k_1, k_2, k_3, k_4, k_5 (assessed from experimental data), and the letter c stands for the "error" factor.

The experiments were carried out utilizing the DoE process of RSM as recommended in [28, 29]. As given in equation (2), the spindle speed, feed rate, radial cut depth, axial depth, and radial rake angle of the tool are the input parameters.

A central composite design (CCD) in statistics is an experimental design that may be used in response surface techniques to create a second-order (quadratic) model of the response variable without requiring a full three-level

factorial experiment. The design matrix is selected as per CCD, and levels are coded as −2, −1, 0, 1, and 2. As per the recommendation and suggestion given by the Production Technology Handbook (Hindustan Machine Tools [30], the ranges of cutting values and conditions are selected as presented in Table 1. As indicated in Table 2, 32 experiments were designed to estimate the process parameters. These experimental designs were developed using the Design-Expert v12 software, which is a tool that helps us in designing experiments and analyzing the data. To anticipate spindle and worktable vibration, a second-order mathematical equation was devised, whose appropriateness was determined using ANOVA [31, 32]. The MATLAB software was used for vibration optimization experiments. The nondominated sorting genetic algorithm (NSGA-II) forecasts spindle and worktable vibration.

4. Experimentation

The milling process was carried out in a CNC vertical machining center (Model-S33). A photographic view of the machined specimen and the HSS tool is shown in Figure 1 and Figure 2. The test specimen of aluminium (Al 6063) alloy with a dimension of 50 mm × 50 mm × 50 mm was prepared as a cube block to perform experimental work. Aluminium 6063 is a medium-strength alloy with moderate fracture toughness at high strength. Aluminium metal's softness, low melting point, and low electrical resistivity are most likely due to the few electrons available for metallic bonding. As a result, considerable attention should be given during machining. Table 2 shows the chemical properties of Al 6063 (Jindal Aluminium, Bengaluru, India). The HSS end mill cutter was used for cutting operations under dry conditions. When compared to other tool steels, HSS tools have greater heat and wear resistance, durability, and hardness levels. HSS has a low coefficient of friction and great shock resistance, which helps to minimize chipping and breakage during use.

While conducting the test, two unidirectional piezoelectric accelerometers were fixed in the spindle to achieve spindle vibration and another on the worktable to achieve worktable vibration. So, the measured vibration in each channel was designated as Channel 1 and Channel 2 as shown in Table 3. The LabVIEW TM software was used in the experiment to act as a data acquisition platform to acquire the vibration.

5. Results and Discussion

5.1. Prediction Using ANOVA. ANOVA is a statistical test that compares the mean values of different groups to determine the influence of one or more factors. The ANOVA test is used in a regression analysis to examine the influence of independent factors on the dependent variable. Moreover, the ANOVA test helps in determining the significance of an experiment's results.

5.2. Prediction of Spindle Vibration Using ANOVA. The spindle vibration was measured using channel 1, whose ANOVA results are shown in Table 4. The F-value is 37.13, and the p value is less than 0.05 indicating that the model is adequate (significant) and there is a 0.01% magnitude chance of occurring due to noise. The lack of fit F-value is 3.11, which indicates that the model term is insignificant and there is an 11.71% chance that the lack of fit F-value is caused by noise. The predicted R^2 of 0.7191 does not match the adjusted R^2 of 0.9589 as closely as one might expect. The S/N ratio is measured by adeq precision. A ratio greater than 4 is preferred. The S/N ratio of 22.034 suggests an adequate signal.

The regression analysis equation of real machining parameters can be expressed as

$$\begin{aligned}\textbf{spindle vibration}\left(\mathbf{A_{SV}}\right) = {} & +0.226242 - 0.000043 \times N - 0.166098 \times fz - 0.172614 \times a_p - 0.248864 \times a_e - 0.001251 \times \gamma \\ & - 0.000025 \times N \times fz + 2.50000E - 06 \times Nva_p + 0.000015 \times \mathrm{N} \times a_e - 5.00E - 07 \times N \times \gamma \\ & + 0.1250 \times fz \times a_p - 0.062500 \times fz \times a_e + 0.006250 \times fz \times \gamma + 0.0250 \times a_p \times a_e + 0.000833 \\ & \times a_p \times \gamma + 0.000417 \times a_e \times \gamma + 8.68182E - 09 \times N^2 + 0.426136 \times fz^2 + 0.092045 \times a_p^2 \\ & + 0.142045 \times a_e^2 + 0.000033 \times \gamma^2. \end{aligned} \tag{3}$$

5.3. ANOVA for the Prediction of Worktable Vibration. In channel 2, the vibrations of the worktable are measured. The ANOVA values of worktable vibration are shown in Table 5. The F-value is 53.04, and p values >0.05 show that the model is adequate (significant) and there is a 0.01% chance of change due to noise. The lack of fit F-value is 0.62 showing that the model is inadequate (not significant) and 71.03% could occur due to noise.

The regression equation of actual machining parameters can be expressed as

Table 1: Process parameters and their levels.

Parameters (input variables)	Notations used	Units	Factorial levels				
			−2	−1	0	1	2
Spindle speed	N	rpm	1500	2000	2500	3000	3500
Rate of feed	f_z	mm/rev	0.04	0.06	0.08	0.1	0.12
Depth of cut (axial)	a_p	mm	0.5	0.6	0.7	0.8	0.9
Depth of cut (radial)	a_e	mm	0.5	0.6	0.7	0.8	0.9
Radial rake angle of tool	γ	Degree	12	15	18	21	24

Table 2: Chemical properties of Al 6063.

Weight (%)	Si	Cu	Fe	Mn	Cr	Mg	Ti	Zn	Al
Al 6063	0.44	0.028	0.21	0.047	0.011	0.48	0.011	0.079	97.70

Figure 1: Experimentation setup.

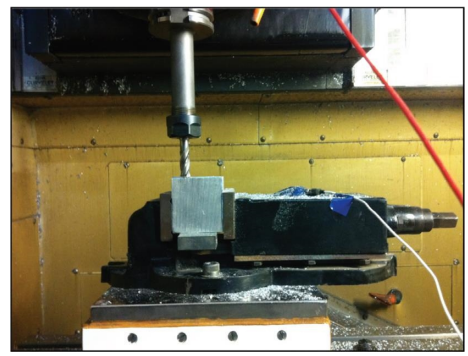

Figure 2: Photographic view of the machined specimen and the HSS tool.

Table 3: Trial (experimental) values with responses.

Run	Machine spindle speed	Rate of feed	Depth of cut (axial)	Depth of cut (radial)	Radial tool rake angle	Channel 1: spindle vibration $A_{SV(Exp)}$	Channel 2: worktable vibration $A_{WTV(Exp)}$	Predicted RSM: spindle vibration $A_{SV(Pred\ RSM)}$ mm/s^2	Predicted RSM: worktable vibration $A_{WTV(Pred\ RSM)}$
1	2000	0.06	0.6	0.6	21	0.019	0.0035	0.0187	0.0035
2	3000	0.06	0.6	0.6	15	0.021	0.0043	0.0206	0.0043
3	2000	0.1	0.6	0.6	15	0.018	0.0035	0.0177	0.0035
4	3000	0.1	0.6	0.6	21	0.018	0.0041	0.0178	0.0041
5	2000	0.06	0.8	0.6	15	0.018	0.0042	0.0176	0.0042
6	3000	0.06	0.8	0.6	21	0.019	0.004	0.0187	0.0040

Table 3: Continued.

Run	Machine spindle speed	Rate of feed	Depth of cut (axial)	Depth of cut (radial)	Radial tool rake angle	Channel 1: spindle vibration $A_{SV(Exp)}$	Channel 2: worktable vibration $A_{WTV(Exp)}$	Predicted RSM: spindle vibration $A_{SV(Pred\ RSM)}$ mm/s^2	Predicted RSM: worktable vibration $A_{WTV(Pred\ RSM)}$
7	2000	0.1	0.8	0.6	21	0.021	0.0041	0.0208	0.0041
8	3000	0.1	0.8	0.6	15	0.02	0.0038	0.0197	0.0038
9	2000	0.06	0.6	0.8	15	0.018	0.004	0.0178	0.0040
10	3000	0.06	0.6	0.8	21	0.021	0.0041	0.0209	0.0041
11	2000	0.1	0.6	0.8	21	0.019	0.004	0.0190	0.0040
12	3000	0.1	0.6	0.8	15	0.021	0.0044	0.0209	0.0044
13	2000	0.06	0.8	0.8	21	0.02	0.0041	0.0199	0.0041
14	3000	0.06	0.8	0.8	15	0.024	0.0032	0.0238	0.0032
15	2000	0.1	0.8	0.8	15	0.018	0.003	0.0179	0.0030
16	3000	0.1	0.8	0.8	21	0.023	0.004	0.0230	0.0040
17	1500	0.08	0.7	0.7	18	0.021	0.0042	0.0214	0.0042
18	3500	0.08	0.7	0.7	18	0.025	0.0046	0.0254	0.0046
19	2500	0.04	0.7	0.7	18	0.015	0.0032	0.0156	0.0032
20	2500	0.12	0.7	0.7	18	0.015	0.0031	0.0152	0.0031
21	2500	0.08	0.5	0.7	18	0.017	0.0042	0.0174	0.0042
22	2500	0.08	0.9	0.7	18	0.019	0.0039	0.0194	0.0039
23	2500	0.08	0.7	0.5	18	0.018	0.0039	0.0189	0.0039
24	2500	0.08	0.7	0.9	18	0.022	0.0038	0.0219	0.0038
25	2500	0.08	0.7	0.7	12	0.015	0.0037	0.0156	0.0036
26	2500	0.08	0.7	0.7	24	0.016	0.0039	0.0162	0.0039
27	2500	0.08	0.7	0.7	18	0.015	0.0035	0.0147	0.0035
28	2500	0.08	0.7	0.7	18	0.015	0.0036	0.0147	0.0035
29	2500	0.08	0.7	0.7	18	0.015	0.0034	0.0147	0.0035
30	2500	0.08	0.7	0.7	18	0.015	0.0035	0.0147	0.0035
31	2500	0.08	0.7	0.7	18	0.014	0.0036	0.0147	0.0035
32	2500	0.08	0.7	0.7	18	0.015	0.0035	0.0147	0.0035

Table 4: ANOVA results of response 1: channel 1 (spindle vibration).

Source	Sum of squares	Df	Mean square	F-value	p value	
Model	0.0003	20	0.0000	37.13	<0.0001	Significant
N	0.000024	1	0.0000	67.02	<0.0001	
f_z	$1.667E-07$	1	$1.667E-07$	0.4654	0.5092	
a_p	$6.000E-06$	1	$6.000E-06$	16.75	0.0018	
a_e	0.0000	1	0.0000	37.70	<0.0001	
γ	$6.667E-07$	1	$6.667E-07$	1.86	0.1997	
$N\ f_z$	$1.000E-06$	1	$1.000E-06$	2.79	0.1229	
$N\ a_p$	$2.500E-07$	1	$2.500E-07$	0.6981	0.4212	
$N\ a_e$	$9.000E-06$	1	$9.000E-06$	25.13	0.0004	
$N\ \gamma$	$9.000E-06$	1	$9.000E-06$	25.13	0.0004	
$f_z a_p$	$1.000E-06$	1	$1.000E-06$	2.79	0.1229	
$f_z a_e$	$2.500E-07$	1	$2.500E-07$	0.6981	0.4212	
$f_z\ \gamma$	$2.250E-06$	1	$2.250E-06$	6.28	0.0292	
$a_p a_e$	$1.000E-06$	1	$1.000E-06$	2.79	0.1229	
$a_p\ \gamma$	$1.000E-06$	1	$1.000E-06$	2.79	0.1229	
$a_e\ \gamma$	$2.500E-07$	1	$2.500E-07$	0.6981	0.4212	
N^2	0.0001	1	0.0001	385.86	<0.0001	
f_z^2	$8.523E-07$	1	$8.523E-07$	2.38	0.1512	
a_p^2	0.0000	1	0.0000	69.40	<0.0001	
a_e^2	0.0001	1	0.0001	165.26	<0.0001	
γ^2	$2.561E-06$	1	$2.561E-06$	7.15	0.0216	
Residual	$3.939E-06$	11	$3.581E-07$			
Lack of fit (LF)	$3.106E-06$	6	$5.177E-07$	3.11	0.1171	Not significant
Error	$8.333E-07$	5	$1.667E-07$			
Cor total	0.0003	31				

Table 5: ANOVA for response 2: channel 2 (worktable vibration).

Source	Sum of squares	df	Mean square	F-value	p value	
Model	$4.778E-06$	20	$2.389E-07$	53.04	<0.0001	Significant
N	$2.204E-07$	1	$2.204E-07$	48.94	<0.0001	
f_z	$2.042E-08$	1	$2.042E-08$	4.53	0.0567	
a_p	$1.838E-07$	1	$1.838E-07$	40.80	<0.0001	
a_e	$3.375E-08$	1	$3.375E-08$	7.49	0.0193	
γ	$1.504E-07$	1	$1.504E-07$	33.40	0.0001	
$N\ f_z$	$2.256E-07$	1	$2.256E-07$	50.09	<0.0001	
$N\ a_p$	$3.306E-07$	1	$3.306E-07$	73.40	<0.0001	
$N\ a_e$	$5.625E-09$	1	$5.625E-09$	1.25	0.2876	
$N\ \gamma$	$1.563E-08$	1	$1.563E-08$	3.47	0.0894	
$f_z a_p$	$3.063E-08$	1	$3.063E-08$	6.80	0.0244	
$f_z a_e$	$1.563E-08$	1	$1.563E-08$	3.47	0.0894	
$f_z\ \gamma$	$1.406E-07$	1	$1.406E-07$	31.22	0.0002	
$a_p a_e$	$5.256E-07$	1	$5.256E-07$	116.70	<0.0001	
$a_p\ \gamma$	$3.906E-07$	1	$3.906E-07$	86.73	<0.0001	
$a_e\ \gamma$	$1.806E-07$	1	$1.806E-07$	40.10	<0.0001	
N^2	$1.339E-06$	1	$1.339E-06$	297.24	<0.0001	
f_z^2	$2.867E-07$	1	$2.867E-07$	63.65	<0.0001	
a_p^2	$4.667E-07$	1	$4.667E-07$	103.62	<0.0001	
a_e^2	$1.700E-07$	1	$1.700E-07$	37.75	<0.0001	
γ^2	$1.188E-07$	1	$1.188E-07$	26.37	0.0003	
Residual	$4.955E-08$	11	$4.504E-09$			
Lack of fit	$2.121E-08$	6	$3.535E-09$	0.6239	0.7103	Not significant
Pure error	$2.833E-08$	5	$5.667E-09$			
Cor total	$4.827E-06$	31				

$$\begin{aligned}\textbf{work table vibration}\left(\mathbf{A_{WTV}}\right) = {} & +0.019316 - 2.38106E-06 \times N - 0.015350 \times fz - 0.006284 \times a_p - 0.005034 \times a_e \\ & - 0.000914 \times \gamma + 0.000012 \times N \times fz - 2.87500E-06 \times N \times a_p - 3.75000E \\ & - 07 \times N \times a_e - 2.08333E-08 \times N \times \gamma - 0.021875 \times fz \times a_p + 0.015625 \times fz \times a_e \\ & + 0.001562 \times fz \times \gamma - 0.018125 \times a_p \times a_e + 0.000521 \times a_p \times \gamma + 0.000354 \times a_e \times \gamma \\ & + 8.54545E-10 \times N - 0.247159 \times fz^2 + 0.012614 \times a_p^2 + 0.007614 \times a_e^2 + 7.07071E \\ & - 06 \times \gamma^2.\end{aligned} \tag{4}$$

Table 6 shows the adjusted R^2 and predicted R^2 values for spindle and worktable vibration. The R^2 value and the predicted R^2 value are 0.9589 and 0.7191 for spindle vibration. The R^2 value and the predicted R^2 value are 0.9711 and 0.8795 for worktable vibration. The R^2 value is 0.9589 for spindle vibration and 0.9711 for worktable vibration. The coefficient of determination R^2 indicates that the goodness of fit for the models is nearer to 1. So, the model is significant.

5.4. Interaction Effect for Spindle Vibration (A_{SV}). Figure 3(a) shows the interaction plot and its effects on the spindle speed and the rate of feed on spindle vibration. Due to the wide contact area between the cutting tool and the workpiece and tool movement relative to the workpiece, an increase in the feed is followed by an increase in spindle vibration. However, when the spindle speed is between 2000 and 3000 rpm, the vibration is relatively low, indicating that a medium spindle speed produces better results. Figure 3(b) depicts the interaction plot of spindle speed and the depth of cut (axial) on spindle vibration. The vibration is low when the spindle speed is between 2000 and 3000 rpm. However, when the depth of cut (axial) is between 0.6 and 0.7 mm, vibration is reduced. This might be because the contact area is damped, resulting in minimal vibration. The interaction impact of spindle speed and radial depth on spindle vibration is depicted in Figure 3(c). As with the depth of cut (axial), the same result occurs. When the radial depth of cut is between 0.7 and 0.8 mm, however, vibration is reduced. This is due to the increased difficulty of moving the tool into the workpiece. The interaction impact of the spindle speed and radial rake angle of the tool on spindle vibration is shown in Figure 3(d).

When the radial rake angle is low, the vibration is very low. This might be because when the rake angle rises, although the speed should be between 2000 and 3000 rpm, the contact area between the tool and the workpiece grows, causing more chips to develop and increased vibration in the

Table 6: Adjusted R^2 and predicted R^2 values for spindle and worktable vibration.

Vibrations	Source	Sequential p value	Lack of fit p value	R^2	Adjusted R^2	Predicted R^2	
Spindle vibration	Quadratic	<0.0001	0.1171	0.9854	0.9589	0.7191	Suggested
Worktable vibration	Quadratic	<0.0001	0.7103	0.9897	0.9711	0.8795	Suggested

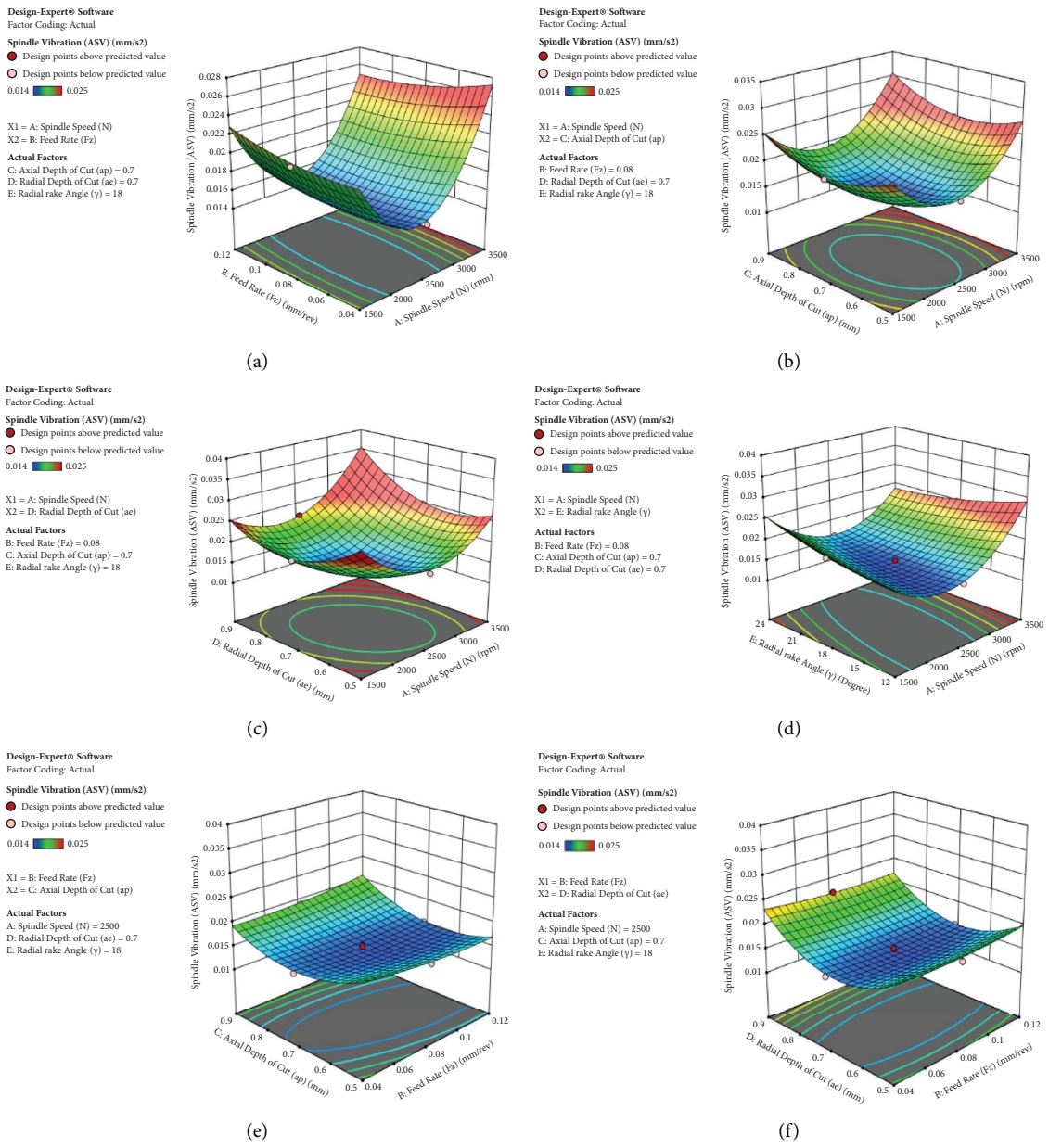

Figure 3: Continued.

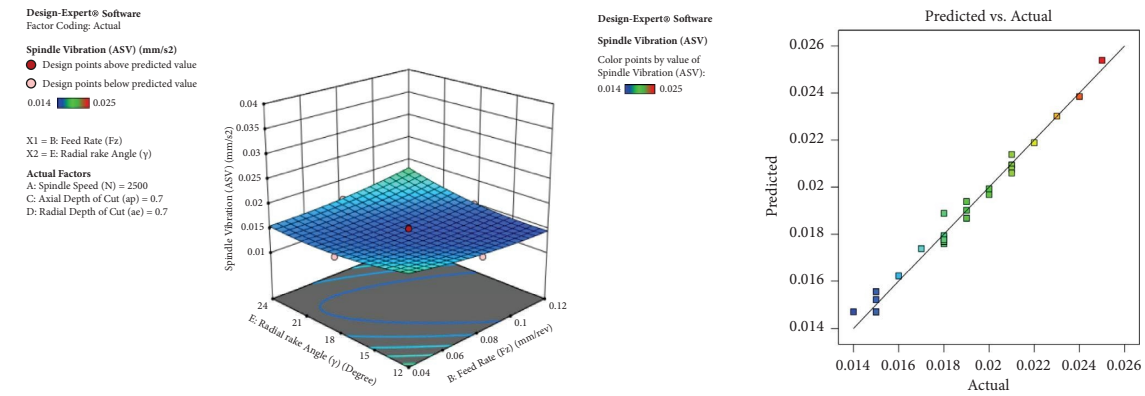

FIGURE 3: Interaction plot for spindle vibration of (a) N vs. f_z over A_{SV}, (b) N vs. a_p over A_{SV}, (c) N vs. a_e over A_{SV}, (d) N vs. γ over A_{SV}, (e) f_z vs. a_p over A_{SV}, (f) f_z vs. a_e over A_{SV}, (g) f_z vs. γ over A_{SV}, and (h) plot of predicted response vs. actual responses (spindle vibration).

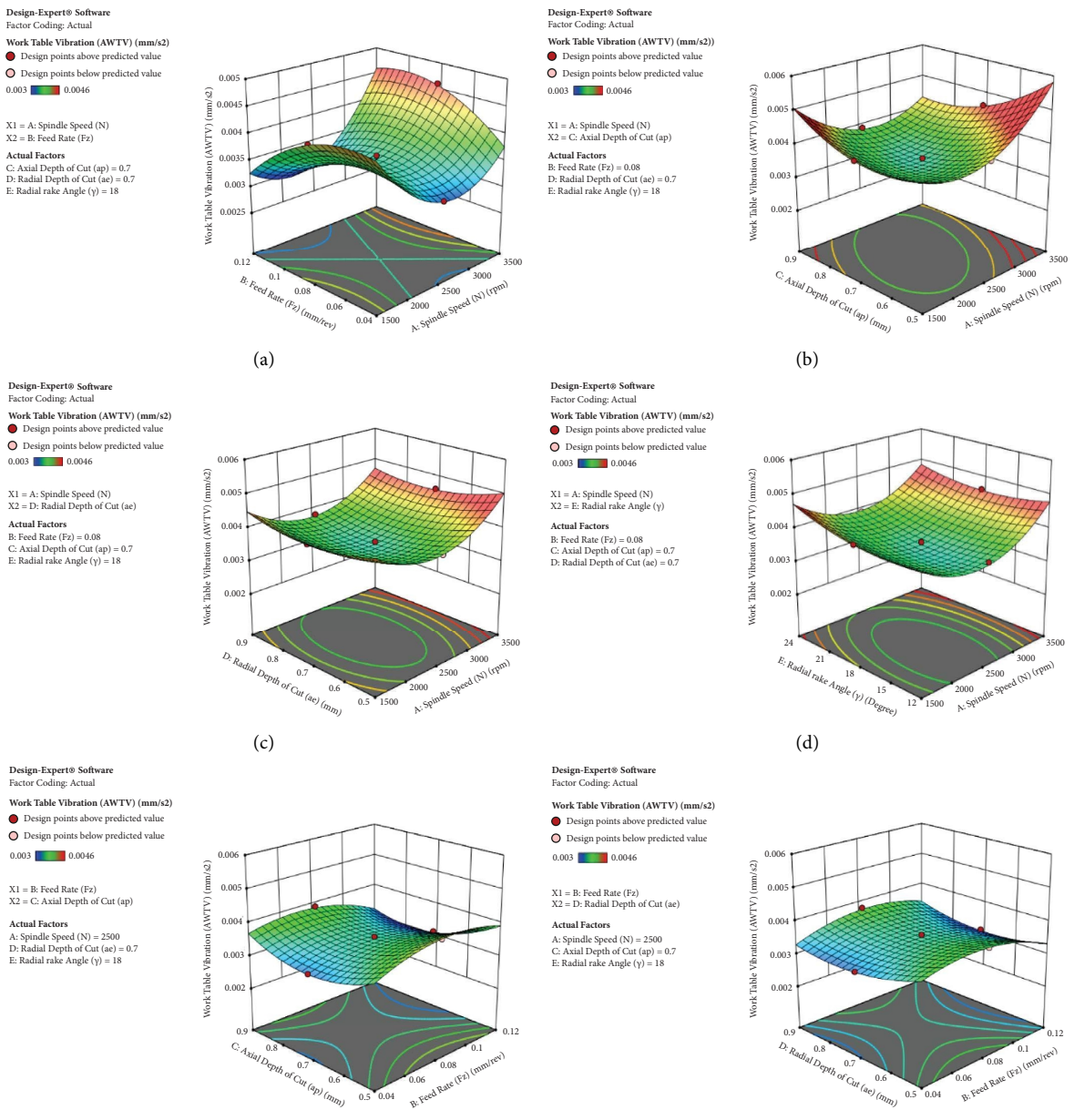

FIGURE 4: Continued.

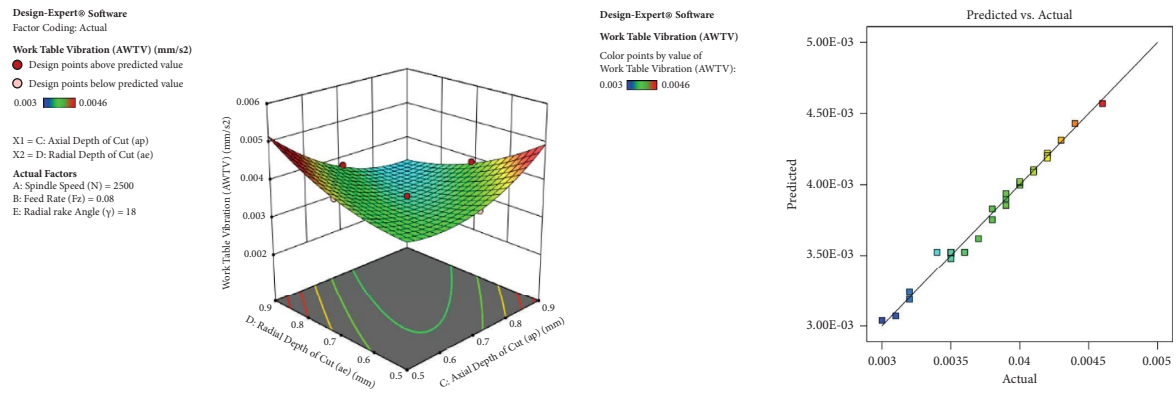

FIGURE 4: Interaction effect for worktable vibration of (a) N vs. f_z over A_{WTV}, (b) N vs. a_p over A_{WTV}, (c) N vs. a_e over A_{WTV}, (d) N vs. γ over A_{WTV}, (e) f_z vs. a_p over A_{WTV}, (f) f_z vs. a_e over A_{WTV}, (g) f_z vs. γ over A_{WTV}, and (h) plot of predicted response vs. actual responses (worktable vibration).

spindle. The interaction impact of the rate of feed and the axial depth of cut on spindle vibration is revealed in Figure 3(e). Figures 3(a) and 3(b) show that when the rate of feed rises, vibration increases and vibration decreases as the axial depth of cut decreases between 0.6 and 0.7 mm. The interaction impact of the rate of feed and the radial depth of cut on spindle vibration is revealed in Figure 3(f). As illustrated in Figures 3(a) and 3(c), the same outcome is duplicated. Figure 3(g) indicates that the rate of feed and the radial rake angle have a less interaction impact. Figure 3(h) depicts a plot of predicted vs. actual responses.

5.5. Interaction Effect for Worktable Vibration (A_{WTV}). Figure 4(a) depicts the interaction effect of the spindle speed and the rate of feed on worktable vibration. The rate of feed has less influence on worktable vibration than the spindle speed. The vibration is at its lowest between 2000 and 2750 rpm, and then, the vibration rises beyond these limits. As previously stated, the spindle vibrations will be more significant at lower and higher speeds, resulting in increased worktable vibrations. These spindle vibrations will be transmitted to the worktable, resulting in vibrations on the work surface. The vibration on the worktable is lessened when the rate of feed is increased. The worktable vibration is high between 0.06 and 0.1 mm/rev. This could be because the spindle dampens most of the vibration frequencies at lower and higher rates of feed, resulting in only minor vibrations in the worktable, whereas at an intermittent rate of feed, the vibrations transferred to the spindle are less and the majority of the vibrations are transferred to the worktable.

The interaction impact of the spindle speed and axial depth of cut on worktable vibration is depicted in Figure 4(b). This case probably occurs due to the spindle vibrating more at lower depths of cut (axial) and higher speeds, and these vibrations are transmitted to the worktable, causing worktable vibrations. Still, there was no discernible effect at higher axial depths. When the spindle speed is low, the change in axial depth has little effect on the vibration of the worktable. The increase in axial depth reduced worktable vibration, while the spindle speed was low between 2000 and 2750 rpm, with a maximum spindle speed of 3500 rpm. This might be due to the fact that even when the axial depth increases, the tool continues to remove material from the workpiece at a consistent rate, even at decreased spindle speeds. Figure 4(c) depicts the interaction influence of the spindle speed and the radial depth of cut-over worktable vibration. The spindle speed should be between 2000 and 2750 rpm, and the radial depth should be between 0.6 and 0.8 mm to reduce worktable vibration. This might be because the spindle vibrates more at lower and greater radial depths, conveying this influence to the worktable as well. The vibrations will be damped at an intermediate value of the radial depth, resulting in low worktable vibrations.

The impact of the spindle speed and rake angle on worktable vibration is shown in Figure 4(d). The worktable vibration was found to be greater at lower rake angles than at higher rake angles. Worktable vibration gets minimum at a rake angle of 15°–17° and a radial depth of 0.70–0.80 mm. Figures 4(e)–4(g) provide less significant graphs of the worktable vibration effects of the axial depth and rate of feed, radial depth and rate of feed, radial rake angle and rate of feed, and axial depth and radial depth, respectively. More radial depth produces a significant increase in worktable vibration at higher rake angles because of more contact between the tool and the workpiece, resulting in increased chatter. Figure 4(h) displays a plot of predicted vs. actual worktable vibration responses.

6. Multiobjective Optimization

The objective of the function needs to be a minimum for optimizing spindle and worktable vibration. As a result, the process becomes complex, and in order to find the optimal solution, one must consider a multiobjective function [29]. To optimize spindle and worktable vibration, the nondominant-based genetic algorithm (NSGA-II) is employed.

FIGURE 5: Performance of fitness value generation and the best and most consistent variable performances in structured form: (a) distance of individuals, (b) average spread of generations, (c) rank histogram of individuals, and (d) GA optimization tool interface.

6.1. Nondominant-Based Genetic Algorithm (NSGA-II). NSGA-II is an effective search strategy. It is driven by natural selection, which is based on Darwin's theory. The NSGA-II approach expands the scope of the search procedure. This approach intended to identify a collection of optimal solutions known as nondominated solutions, also known as the Pareto set. A nondominated solution is one that delivers an appropriate balance between all objectives without degrading any of them.

NSGA-II was used in this work to achieve multiobjective optimization with parameter constraints. The constructed regression model is used by a genetic algorithm to anticipate the ideal relationship between cutting parameters. The output responses are spindle vibration and worktable

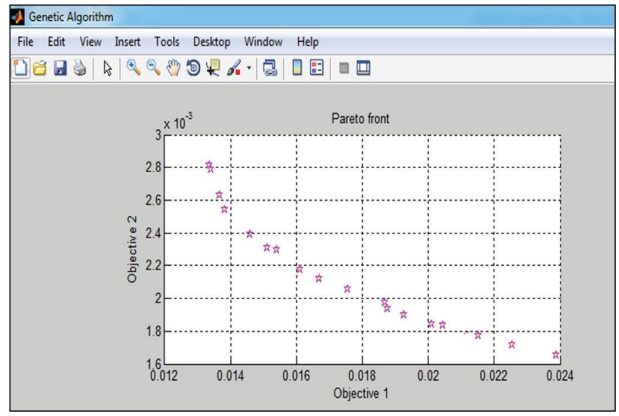

Figure 6: Chart of the Pareto-optimum frontier.

Table 7: Pareto-optimum solutions (NSGA-II).

Sl. no.	N	f_z	a_p	a_e	γ	Spindle vibration: predicted by NSGA-II $ASV_{(NSGA\text{-}II)}$	Worktable vibration: predicted by NSGA-II $AWTV_{(NSGA\text{-}II)}$
1	2326.98	0.11	0.89	0.89	12.06	0.02404	0.00167
2	2324.31	0.12	0.89	0.89	12.06	0.02388	0.00165
3	2300.28	0.12	0.70	0.79	12.23	0.01450	0.00264
4	2288.40	0.17	0.70	0.69	12.47	0.01339	0.00284
5	2308.64	0.12	0.81	0.78	12.35	0.01599	0.00226
6	2320.46	0.12	0.88	0.85	12.07	0.02120	0.00177
7	2295.81	0.12	0.70	0.70	12.39	0.01336	0.00281
8	2316.22	0.12	0.84	0.78	12.24	0.01696	0.00214
9	2321.88	0.12	0.88	0.86	13.07	0.02199	0.00191
10	2299.54	0.12	0.79	0.76	12.26	0.01510	0.00231
11	2306.80	0.12	0.82	0.79	12.20	0.01670	0.00212
12	2289.54	0.12	0.70	0.70	12.40	0.01337	0.00282
13	2313.43	0.12	0.81	0.85	12.46	0.01866	0.00207
14	2322.56	0.12	0.85	0.84	12.07	0.01926	0.00190
15	2325.76	0.12	0.89	0.80	12.04	0.02391	0.00166
16	2318.48	0.12	0.87	0.82	12.57	0.01950	0.00198
17	2320.19	0.12	0.85	0.86	12.08	0.02034	0.00187
18	2300.56	0.12	0.76	0.73	12.24	0.01421	0.00247
19	2305.43	0.11	0.83	0.81	12.62	0.01761	0.00210
20	2319.12	0.12	0.77	0.76	12.12	0.01467	0.00239
21	2307.26	0.12	0.74	0.71	12.19	0.01367	0.00263

Table 8: Validation of the model.

Trail no.	Machine spindle speed	Rate of feed	Depth of cut (axial)	Depth of cut (radial)	Radial tool rake angle	Spindle vibration (optimized)	Spindle vibration (observed)	Error %	Worktable vibration (optimized)	Worktable vibration (observed)	Error %
1	2300	0.1	0.6	0.5	21	0.01631	0.016	1.90	0.00301	0.0030	0.33
2	2200	0.12	0.7	0.6	18	0.01789	0.018	−0.61	0.00367	0.0036	1.90
3	2600	0.04	0.5	0.5	12	0.01422	0.014	1.54	0.00326	0.0033	−1.23

vibration; the MATLAB 2013a software was used for optimization purposes to optimize the vibration. The input objective function utilizes the MOGA methodology [33, 34]:

$$\begin{aligned}&\text{to minimize: spindle vibration } (A_{\mathrm{SV}}): A_{\mathrm{SV}}\left(N, f_z, a_p, a_e, \gamma\right),\\ &\text{to minimize: worktable vibration } (A_{\mathrm{WTV}}): A_{\mathrm{WTV}}\left(N, f_z, a_p, a_e, \gamma\right) \text{ subject to constraints: } A_{\mathrm{SV}} \le A_{\mathrm{SV}} \text{ limit}, A_{\mathrm{WTV}} \le A_{\mathrm{WTV}} \text{limit},\end{aligned} \tag{5}$$

where A_{SV} and A_{WTV} limitations define the lower and upper limits that must be fulfilled. Among parameter ranges,

$$\begin{aligned}&1500 \le \text{spindle speed of the machine } (N) \le 3500\text{rpm},\\ &0.04 \le \text{rate of feed } \left(f_z\right) \le 0.12\ \frac{\text{mm}}{\text{rev}},\\ &0.5 \le \text{depth of cut (axial)} \left(a_p\right) \le 0.9\text{mm},\\ &0.5 \le \text{depth of cut (radial)} \left(a_e\right) \le 0.9\text{mm},\\ &12 \le \text{radial rake angle of tool } (\gamma) \le 24 \text{ degree}.\end{aligned} \tag{6}$$

To achieve the best results, the following conditions were used:

(i) A population size of 100
(ii) A population-type vector
(iii) A scaling function rank of function
(iv) Stochastic uniform crossover,
(v) A Gaussian mutation function
(vi) A mutation rate of 0.1
(vii) A scattered mutation function
(viii) A crossover rate of 1.0
(ix) A generation size of 1000

Figure 5 displays in coded form the performance of fitness value creation and the best individual variable performances. Figure 6 displays the Pareto-optimal frontier scattered points for their results as a consequence of NSGA-II optimization conducted using MATLAB software. The input parameter grouping of twenty-one sets of nondominated Pareto-optimal solutions based on the NSGA-II analysis is shown in Table 7. The spindle vibration ranged from 0.02404 to 0.01336 mm/s^2, while the worktable vibration ranged from 0.00284 to 0.00165 mm/s^2. Table 6 shows that all of the NSGA-II generated solutions have an equal high level of agreement. According to the research results, all of the solutions created by NSGA-II are equally good. The selection of Pareto-optimal solutions helps the manufacturing engineer's and researchers' expectations.

7. Validation of the Model

Table 8 demonstrates that a regression model developed through RSM of DoE utilizing CCD was validated using a confirmatory test. Vibration of both the spindle speed and the worktable is compared between values predicted by NSGA-II and experimental values. The percentage of error is determined to be within ±2%, confirming the model's validity.

8. Conclusion

Based on the designed experiments, utilizing central composite design, the spindle vibration, and worktable vibration in terms of acceleration amplitude, the experiment is performed on aluminium 6063 using an HSS tool in a CNC milling machine. The ANOVA technique was used to examine performance characteristics. The machining variables and their responses are optimized by NSGA-II.

Spindle speed is an important factor in increasing spindle vibration amplitude. To ensure lesser vibration, the spindle speed should be between 2000 and 2800 rpm. In addition to spindle speed, the axial depth of the cut is an important element that contributes to vibration. The axial depth of the incision should be between 0.7 and 0.8 mm to guarantee low vibration. The cut's radial depth should be between 0.7 and 0.8 mm. The radial rake angle should be between 12° and 18° for low vibration, and the feed rate should be between 0.04 and 0.08 mm/rev.

The smallest worktable vibration was achieved by using spindle speeds ranging from 2000 to 3000 rpm, feed rates ranging from 0.1 to 0.12 mm/rev, axial depth of cut ranging from 0.5 to 0.7 mm, radial depth of cut ranging from 0.6 to 0.8 mm, and radial rake angles ranging from 15° to 18°.

MATLAB provided 21 nondominated Pareto-optimal solutions based on multiobjective optimization using the nondominated sorted genetic algorithm (NSGA-II). The result obtained from NSGA-II is reasonably excellent. The suggested hybrid approach minimizes the cost and reduction of vibration amplitude prediction for real-world machining conditions.

The future direction of this research will be use of a carbide-cutting tool to conduct machining operations with respect to tool wear and surface roughness, as well as conducting the experiment based on measurement of the cutting force.

Data Availability

The data used to support the findings of this study are included in the article.

Disclosure

The major part of this study was performed as a part of the employment of Wollega University, Nekemte, Ethiopia.

Conflicts of Interest

The authors declare that there are no conflicts of interest regarding the publication of this article.

Authors' Contributions

Hirpa G. Lemu was proposed the methodology. Endalkachew Mosisa Gutema, Mahesh Gopal, and Jaleta Sori performed experiments and data analysis. Endalkachew Mosisa Gutema and Mahesh Gopal provided software. Mahesh Gopal wrote the original draft of the manuscript. Endalkachew Mosisa Gutema, Hirpa G. Lemu, and Jaleta Sori reviewed and edited the manuscript. All the authors have read and agreed to the published version of the manuscript.

Acknowledgments

The authors highly appreciate the financial support provided by the collaboration project INDMET (Grant no. 62862) funded by the NORHED II program.

References

[1] Y. Guo, B. Lin, and W. Wang, "Modeling of cutting forces with a serrated end mill," *Mathematical Problems in Engineering*, vol. 2019, Article ID 1796926, 13 pages, 2019.

[2] S. Orhan, A. O. Er, N. Camuşcu, and E. Aslan, "Tool wear evaluation by vibration analysis during end milling of AISI D3 cold work tool steel with 35 HRC hardness," *NDT and E International*, vol. 40, no. 2, pp. 121–126, 2007.

[3] I. Yesilyurt and H. Ozturk, "Tool condition monitoring in milling using vibration analysis," *International Journal of Production Research*, vol. 45, no. 4, pp. 1013–1028, 2007.

[4] H. Ding, R. Ibrahim, K. Cheng, and S. J. Chen, "Experimental study on machinability improvement of hardened tool steel using two-dimensional vibration-assisted micro-end-milling," *International Journal of Machine Tools and Manufacture*, vol. 50, no. 12, pp. 1115–1118, 2010.

[5] P. S. Sivasakthivel, V. Velmurugan, and R. Sudhakaran, "Prediction of vibration amplitude from machining parameters by response surface methodology in end milling," *The International Journal of Advanced Manufacturing Technology*, vol. 53, no. 5–8, pp. 453–461, 2011.

[6] X. H. Shen, J. Zhang, D. X. Xing, and Y. Zhao, "A study of surface roughness variation in ultrasonic vibration-assisted milling," *The International Journal of Advanced Manufacturing Technology*, vol. 58, no. 5–8, pp. 553–561, 2012.

[7] A. N. Amin, M. H. B. M. Saad, and M. D. Arif, "Modeling and optimization of surface roughness and vibration amplitude in heat assisted end milling of SKD 11 tool steel using ball nose tool," *Advanced Materials Research*, vol. 538-541, pp. 799–803, 2012.

[8] M. M. De Aguiar, A. E. Diniz, and R. Pederiva, "Correlating surface roughness, tool wear and tool vibration in the milling process of hardened steel using long slender tools," *International Journal of Machine Tools and Manufacture*, vol. 68, pp. 1–10, 2013.

[9] V. Ostasevicius, R. Gaidys, R. Dauksevicius, and S. Mikuckyte, "Study of vibration milling for improving the surface finish of difficult-to-cut materials," *Strojniski Vestnik/Journal of Mechanical Engineering*, vol. 59, no. 6, pp. 351–357, 2013.

[10] G. Zhang, J. Li, Y. Chen, Y. Huang, X. Shao, and M. Li, "Prediction of surface roughness in end face milling based on Gaussian process regression and cause analysis considering tool vibration," *The International Journal of Advanced Manufacturing Technology*, vol. 75, no. 9–12, pp. 1357–1370, 2014.

[11] S. S. Bhogal, C. Sindhu, S. S. Dhami, and B. S. Pabla, "Minimization of surface roughness and tool vibration in CNC milling operation," *Journal of Optimization*, vol. 2015, Article ID 192030, 13 pages, 2015.

[12] P. S. Sivasakthivel, R. Sudhakaran, and S. Rajeswari, "Optimization and sensitivity analysis of geometrical and process parameters to reduce vibration during end milling process," *Machining Science and Technology*, vol. 21, no. 3, pp. 452–473, 2017.

[13] P. S. Paul, C. K. Shobhan Kumar, M. Joshua, S. Vignesh, S. Saravanan, and A. S. Varadarajan, "Study on the influence of magnetorheological fluid on tool vibration during end milling process," *International Journal of Dynamics and Control*, vol. 5, no. 3, pp. 696–703, 2017.

[14] T. Huang, X. M. Zhang, and H. Ding, "Tool orientation optimization for reduction of vibration and deformation in ball-end milling of thin-walled impeller blades," *Procedia CIRP*, vol. 58, pp. 210–215, 2017.

[15] A. Susanto, C. H. Liu, K. Yamada, Y. R. Hwang, R. Tanaka, and K. Sekiya, "Application of Hilbert–Huang transform for vibration signal analysis in end-milling," *Precision Engineering*, vol. 53, pp. 263–277, 2018.

[16] S. Wojciechowski, R. W Maruda, G. M Krolczyk, P. Niesłony, and P. Niesłony, "Application of signal-to-noise ratio and grey relational analysis to minimize forces and vibrations during precise ball-end milling," *Precision Engineering*, vol. 51, pp. 582–596, 2018.

[17] M. Luo and Q. Yao, "Vibrations of flat-end cutter entering workpiece process: modeling, simulations, and experiments," *Shock and Vibration*, vol. 2018, Article ID 8419013, 23 pages, 2018.

[18] A. Agic, M. Eynian, J. E. Ståhl, and T. Beno, "Experimental analysis of cutting-edge effects on vibrations in end milling," *CIRP Journal of Manufacturing Science and Technology*, vol. 24, pp. 66–74, 2019.

[19] M. Zhang, D. Zhang, D. Geng, Z. Shao, Y. Liu, and X. Jiang, "Effects of tool vibration on surface integrity in rotary ultrasonic elliptical end milling of Ti–6Al–4V," *Journal of Alloys and Compounds*, vol. 821, Article ID 153266, 2020.

[20] Y. C. Lin, K. Wu, J. P Hung, W. C. Shih, P. K. Hsu, and J. P. Hung, "Prediction of surface roughness based on cutting parameters and machining vibration in end milling using regression method and artificial neural network," *Applied Sciences*, vol. 10, no. 11, p. 3941, 2020.

[21] M. Z. Zahaf and M. Benghersallah, "Surface roughness and vibration analysis in end milling of annealed and hardened bearing steel," *Measurement: Sensors*, vol. 13, Article ID 100035, 2021.

[22] A. A. A. Sonief, A. N. Fauzan, and F. A. Alamsyah, "Evaluation of aluminum surface roughness in the slot end-mill process with variable helix angle," *IOP Conference Series:*

Materials Science and Engineering, vol. 494, no. 1, Article ID 012045, 2019.

[23] L. Ma, I. Howard, M. Pang, Z. Wang, and J. Su, "Experimental investigation of cutting vibration during micro-end-milling of the straight groove," *Micromachines*, vol. 11, no. 5, p. 494, 2020.

[24] S. Gowthaman and T. Jagadeesha, "Comparative study on the critical effect of radial rake angle and machining parameters on the formation of vibration amplitude during end milling of Nimonic 263," *Sādhanā*, vol. 46, no. 4, Article ID 191, 2021.

[25] F. Ahmed, T. J. Ko, R. Kurniawan, and Y. Kwack, "Machinability analysis of difficult-to-cut material during ultrasonic vibration-assisted ball-end milling," *Materials and Manufacturing Processes*, vol. 36, no. 15, pp. 1734–1745, 2021.

[26] Y. Hui, X. Mei, G. Jiang, T. Tao, C. Pei, and Z. Ma, "Milling tool wear state recognition by vibration signal using a stacked generalization ensemble model," *Shock and Vibration*, vol. 2019, Article ID 7386523, 16 pages, 2019.

[27] G. Mahesh, S. Muthu, and S. R. Devadasan, "Prediction of surface roughness of end milling operation using genetic algorithm," *The International Journal of Advanced Manufacturing Technology*, vol. 77, no. 1–4, pp. 369–381, 2015.

[28] D. Montgomery, *Design_Mont_Part1.Pdf*, John Wiley and Sons, Hoboken, NJ, USA, 10th edition, 2001.

[29] R. Suresh Kumar, S. Senthil Kumar, K. Murugan et al., "Optimization of CNC end milling process parameters of low-carbon mold steel using response surface methodology and grey relational analysis," *Advances in Materials Science and Engineering*, vol. 2021, Article ID 4005728, 11 pages, 2021.

[30] Hindustan Machine Tools (Hmt), *Hindustan Machine Tools (HMT) (2001) Production Technology*, Tata McGraw-Hill Education, New York, NY, USA, 2001.

[31] G. C. Verma and P. M. Pandey, "Machining forces in ultrasonic vibration assisted end milling," *Ultrasonics*, vol. 94, pp. 350–363, 2019.

[32] A. Al-Shayea, F. M. Abdullah, M. A. Noman, H. Kaid, and E. Abouel Nasr, "Studying and optimizing the effect of process parameters on machining vibration in turning process of AISI 1040 steel," *Advances in Materials Science and Engineering*, vol. 2020, Article ID 5480614, 15 pages, 2020.

[33] M. Gopal, "Experimental investigation of duplex stainless steel using RSM and multi-objective genetic algorithm (MOGA)," in *Lecture Notes in Mechanical Engineering*, G. R. Santhakumar Mohan and S. Shankar, Eds., pp. 813–834, Springer Nature Singapore Pte Ltd, Singapore, 2021.

[34] J. H. Shaik and S. J, "Optimal selection of operating parameters in end milling of Al-6061 work materials using multi-objective approach," *Mechanics of Advanced Materials and Modern Processes*, vol. 3, no. 1, p. 5, 2017.